



Ultrasonic study of UO_2 : effects of porosity and grain size on ultrasonic attenuation and velocities

D. Laux^{a,*}, B. Cros^a, G. Despaux^a, D. Baron^{b,c}

^a *LAIN UMR CNRS 5011, Université Montpellier 2, 34095 Montpellier cedex 05, France*

^b *EDF, Division Recherches et Développement, 77250 Moret/Loing, France*

^c *CEA Cadarache DEC/SECS., 13108 Saint-Paul-lez-Durance, France*

Received 17 January 2001; accepted 6 November 2001

Abstract

Ultrasonic techniques applied to nuclear fuel characterisation are developed in our group since 1996. Before applying our methods to irradiated fuel, we are searching sensitive parameters which could give interesting information. That is the reason why only results concerning non-irradiated UO_2 are presented. This paper mainly deals with the investigation of a relevant acoustic parameter: the attenuation. Indeed, the ultrasonic attenuation in UO_2 as a function of the operating ultrasonic frequency has been measured on samples with various microstructures: variable fraction volume porosity (1–6%) and grain size (10–90 μm). Using a 15 MHz operating frequency, no attenuation has been observed. With frequencies around 40 MHz, we show that the measured ultrasonic attenuation is only sensitive to grain size (no effect of porosity has been observed). On the contrary, the ultrasonic velocities (which are very sensitive to porosity) are not affected by the sizes of the grains. These reversed and non-correlated effects constitute an interesting tool for UO_2 study because two aspects of the microstructure can be studied separately with ultrasonic waves. © 2002 Elsevier Science B.V. All rights reserved.

PACS: 62-20; 81-70; 28.50

1. Introduction

The thermo-mechanical codes, used to predict the in pile behaviour of the nuclear fuel rods are provided with the different material properties. These properties are evolving strongly and non-uniformly within the fuel pellet, depending on the local fission density and the local temperature history. High burn-up fuel pellets have been widely investigated in the recent past in order to better characterise these kind of materials. Investigations have been particularly focused on the so-called 'rim' region in the pellet periphery. In this region, the ^{238}U self shielding effect leads to the formation of plu-

onium resulting in a fission density twice higher than in the rest of the fuel pellet and consequently to a higher irradiation damage. The damage accumulation leads above a local burn-up threshold to a material restructuring in order to relax the internal constraints. This is characterised by a large set-up of micrometric pores filled by fission gases and a grain subdivision [1,2].

Concerning the determination of the mechanical properties, classical methods efficient for non-irradiated materials, are no more applicable on irradiated fuel pellets because of the pellet fracturation and the large radial gradient in the material properties. As soon as the fuel is in operation, the thermal stresses induces cracks. The pellet cracking pattern is partly random due to the initial material non-homogeneity. The pellet is subdivided in about 18–24 pieces not larger than 5 mm. The fabrication porosity disappears partly and the remaining

* Corresponding author.

E-mail address: laux@lain.univ-montp2.fr (D. Laux).

porosity participates to the fission gases trapping. Non-soluble fission products such as molybdenum, barium, palladium precipitate under the form of metallic and ceramic inclusions; many fission products can enter in the fluorite matrix and create solid solutions. Furthermore, many point defects (vacancies and interstitial) or dislocations loops are created [3]. All these phenomena resulting in a lattice disorder increase affect the propagation of ultrasonic waves. As a result, the use of local acoustic measurements propose an alternative and adequate methodology.

In our previous studies [4,5], laws have been established concerning the effect of porosity volume fraction on ultrasonic velocities and mechanical properties of non-irradiated fuel. These local measurements which agree with global measurements of several authors have focused on the efficiency of acoustic methods. To carry on with the study, new measurements concerning the Rayleigh and longitudinal wave attenuation have been performed on samples with variable grain sizes.

The main goal of this paper is to show how the use of attenuation measurements can provide new information on UO_2 microstructure and that the coupling between attenuation and velocity measurements could constitute a powerful tool for irradiated fuel studies which are planned for the future.

2. Experimental methods

Ultrasonic measurements provide information on sound velocities and attenuation coefficients. In an isotropic material such as sintered UO_2 , two volumic acoustic modes exist: longitudinal and transverse. Other, such as Rayleigh one, can appear in some particular conditions. With the measurement of the velocities of these ultrasonic waves and using some relationships, the evaluation of the elastic constants of the material is possible. If velocity measurements are well known, ul-

trasonic attenuation is a more complex physical phenomenon because it is made up with many processes: intrinsic absorption due to relaxation, diffusion by surface defects, bulk diffusion by grains [6] and pores.

To perform both velocities and attenuation measurements, the use of a special device which is able to work in various modes is necessary because we want to measure many physical parameters. For instance, velocity measurements are performed in time domain and attenuation measurements in frequency domain. Furthermore, if focused sensors are used to work on Rayleigh waves, with the acoustic microscope, longitudinal experiments are performed with planar sensors with the help of a ‘microechograph’.

2.1. Elements of acoustic microscopy [7]

The acoustic microscope used to obtain pictures and to perform Rayleigh wave studies is composed of a sensor which focuses the ultrasonic wave produced by a piezoelectric crystal on the sample, and an electronic system controller. For example, the diameter of a 15 MHz sensor’s lens is 5 mm and the aperture angle is 50° . If higher frequencies are used (for instance 500 MHz), the lens diameter can reach $100\ \mu\text{m}$ (see Fig. 1).

This microscope can be used in different ways:

- *Surface imaging:* the ultrasonic beam is focused on the surface. As the reflected signal depends on the elastic properties of the zone, an image is obtained with an X – Y scan. The resolution can reach a few micrometers at high frequency (500 MHz).
- *Quantitative measurements (acoustic signature $V(z)$):* the sensor is defocused on Z axis. A surface wave called leaky-Rayleigh wave then propagates on the surface of the sample and creates interference with the specular ray coming from the sensor. The pseudo-periodic signal obtained (acoustic signature) is treated and the Rayleigh wave velocity deduced.

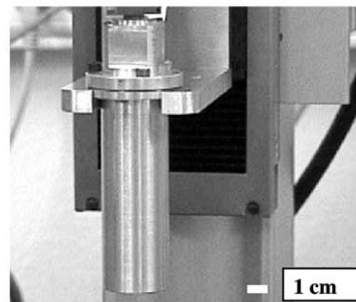
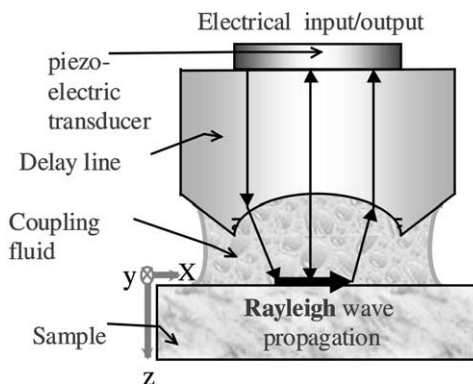


Fig. 1. Schematic representation of an acoustic sensor and photography of a 15 MHz sensor.

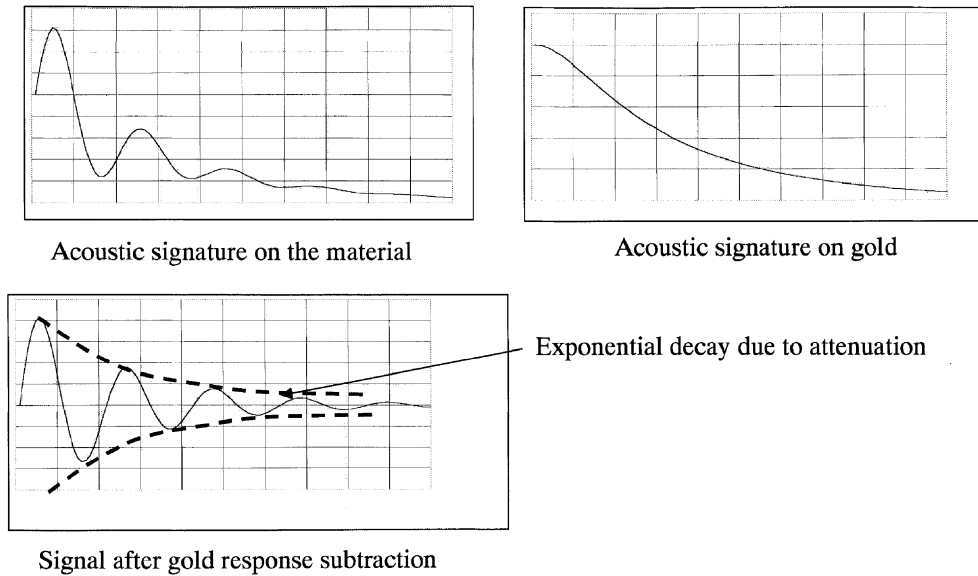


Fig. 2. Experimental measurement of Rayleigh wave attenuation.

- *Contrast imaging*: the image is performed with a small defocusing called Z_d . At each point of acquisition, the Rayleigh wave is generated and the amplitude of the signal received by the sensor is $V(Z_d)$. If two zones of the sample have very different mechanical properties, the period of their $V(z)$ are also very different. As a consequence, $V(Z_d)$ varies a lot between two locations and the contrasts are highly emphasised.
- *Rayleigh wave attenuation measurements*: many ways can be used to evaluate the attenuation of the Rayleigh mode. The first uses the amplitude of the Rayleigh mode peak in the FFT of the $V(z)$. We can also count how many peaks are present in the acoustic signature ($V(z)$). These two methods give a relative evolution between different samples but cannot provide quantitative results. A third method (more accurate) has been used in this paper. The acoustic signature can be represented by the sum of two terms [8]. The first, written Ae^{-bz} is the lens function. It represents the loss of signal due to the defocusing. The second, written $Ce^{-\alpha z} \cos(wz)$ contains the attenuation of the Rayleigh wave (α parameter) and the oscillations due to the interference ($\cos(wz)$ term). As the ultrasonic waves propagate from the lens to the sample through a coupling fluid, α is the sum of two terms: the first represents a loss in the sample and the second a loss due to the density of the coupling fluid. In our experiment, we are using ethanol. As its density is very small compared to this of depleted UO_2 ($\rho = 10960 \text{ kg m}^{-3}$), the loss will not be taken into account. The assessment of α (in dB/mm

for instance) is performed as follows: we subtract the lens function to the acoustic signature and we fit the decrease of the resulting signal. The lens function is acquired on gold: on this material, the critical angle of the surface wave generation is so high that the Rayleigh wave does not appear. Hence, the experimental acquisition is only Ae^{-bz} . A summary of the whole procedure is given on Fig. 2.

As the experimental procedure is complex, giving an absolute accuracy is quite difficult. But, if the measurement on the same sample is performed many times, the relative error mainly due to noise contribution is about 1 dB/mm.

2.2. Microechography

If longitudinal velocities measurements with echography are very well known, they are generally performed on a large zone (about one centimetre) at low frequency. The interest of our method is to work at low frequencies on very small zones. The sensors, calculated and designed in our laboratory operate at about 40 MHz on a zone smaller than the millimetre. They are slightly focused (5°) to correct the small divergence of the beam through the water.

In a previous study [4], we have presented the measurements of longitudinal velocity and thickness of UO_2 sample by a transmission method. If this method is accurate on non-irradiated UO_2 (in which attenuation is small), we do not know at present the result on irradiated UO_2 . Indeed, if d is the thickness of the sample, we

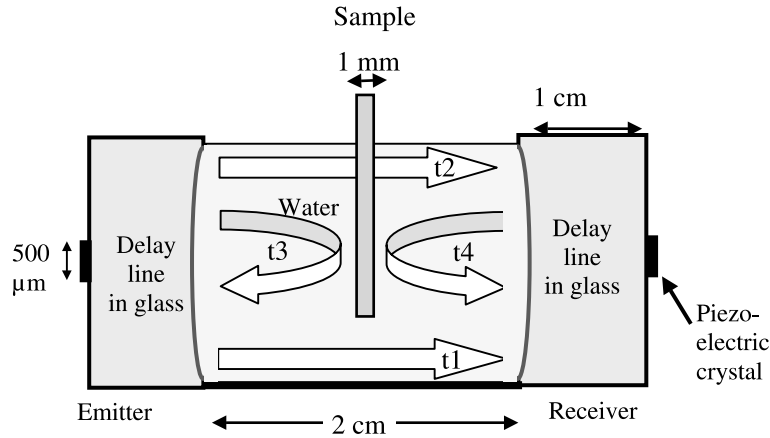


Fig. 3. Ultrasonic travels considered in microechography (schematic representation).

have to use a signal which has propagated $2d$ in the sample. If the attenuation is too high, the analysis of the signal will be tricky. To avoid this problem we have developed a different method (see Figs. 3 and 4).

Notations

- t_1 flight time of transmitted signal in water
- t_2 flight time of transmitted signal in water and sample
- t_3 and t_4 flight times of reflected echoes
- Δt_{ij} $t_i - t_j$
- V_c ultrasonic velocity in the coupling fluid (1500 m s^{-1} in water)

Using these notations we calculate the longitudinal velocity (V_L) and the thickness (d) as follows:

$$d = \frac{1}{2}(\Delta t_{13} + \Delta t_{14})V_c, \tag{1}$$

$$V_L = \frac{dV_c}{d - \Delta t_{12}V_c}. \tag{2}$$

The previous configuration can also be used to measure the longitudinal attenuation. Indeed, after the acquisition of the signals, depending on the signal processing, many information can be obtained. For the velocities measurements, the propagation times (Δt_{ij}) are calculated using the inter-correlation method [9]. If the Fast Fourier Transform algorithms are applied, the longitudinal attenuation is calculated as follows [10].

If $S(\omega)_s$ is the FFT of the signal transmitted through the sample, $S(\omega)_w$ the FFT of the signal transmitted through the water, and I the transmission power of the sample, then

$$\alpha_L(\text{dB/mm}) = -\frac{1}{d} 10 \log \left(\frac{|S(\omega)_s|^2}{|S(\omega)_w|^2 I^2} \right). \tag{3}$$

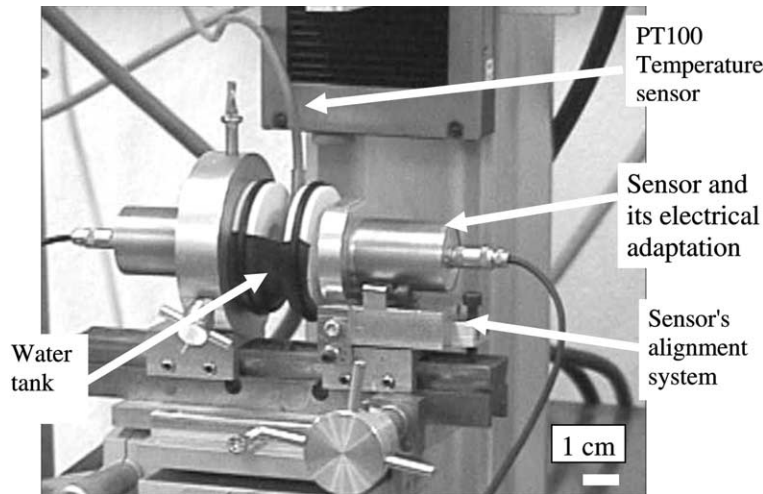


Fig. 4. Photography of the microechographic device.

In this expression, the ultrasonic attenuation in water (which is small) and the sensor diffraction losses are not taken into account. Indeed, we measure a relative variation of the attenuation between different samples using the same experimental device. To perform accurate echographic measurements, our sensors generate very short echoes and have large spectrum. As a result, attenuation is obtained on a large frequency domain (about 40 MHz).

The relative accuracy of the measurement is 0.5 dB/mm, mainly due to the imprecision on F .

3. Experimental results

First, a very high frequency (570 MHz) picture has been made on the 90 μm grains sample with a small defocusing in order to emphasise the contrast and to see the grains without any chemical attack. The picture is presented on Fig. 5. The important contrasts underline high variations in mechanical properties between the grains. Consequently, for studies at smaller frequencies (15 and 40 MHz), the two conditions of ultrasonic scattering (small size of grains compared to the wavelength and random orientation) are verified.

First, the Rayleigh wave attenuation has been measured using the method described in paragraph 2.1 with a 15 MHz ultrasonic sensor. No significant variation has been observed in attenuation versus the size of the grains. As this sensor presents powerful harmonics, it has been used to work at 45 MHz. The quality of the 45 MHz echo has been emphasised by electrical impedance adaptation. The results are presented on Fig. 6.

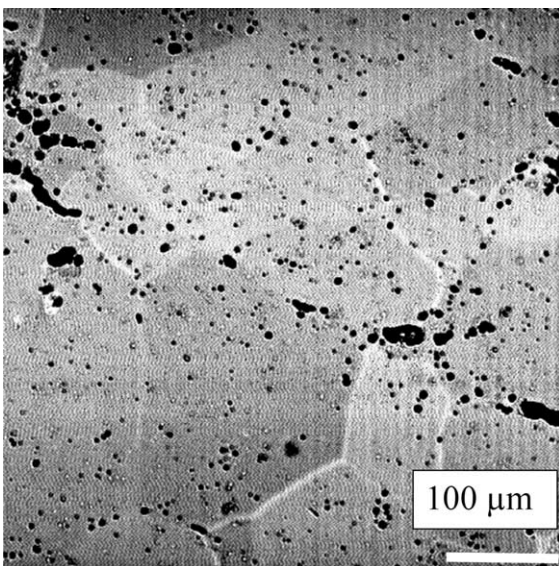


Fig. 5. 570 MHz picture of the 90 μm grain size sample.

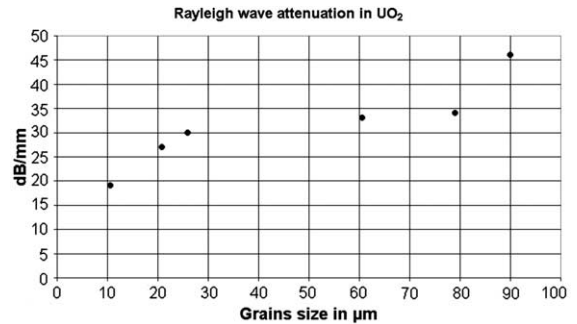


Fig. 6. Rayleigh wave attenuation measured in UO₂ as a function of grain size.

Concerning the longitudinal wave attenuation, it is usually quite small compared to the Rayleigh wave attenuation. Furthermore, we have noticed that its variation as a function of the grain size was not very high. That is the reason why on Fig. 7 only the results obtained for the two extreme values of grain sizes are presented for more clarity. For the 90 μm sample, the value obtained at 20 MHz seems relatively high. Such an element is not very surprising: indeed, even if our sensors can work from 20 to 60 MHz, their efficiency is not very good for low frequencies. A smoothing average has been performed around 20 MHz to suppress the noise effects. For example, if no smoothing is performed on the 10.6 μm sample, some points are under zero which is impossible. Consequently, the results between 20 and 30 MHz have to be carefully considered.

Using Papadakis' model [6], we have tried to check the accuracy of our experimental approach. The predicted values of attenuation are qualitatively in good agreement with the experiments. For instance, for the longitudinal attenuation, the theory predicts a variation of 1 dB/mm for grain sizes of 10 μm for the considered frequencies and a variation of 6 dB/mm for large grains (90 μm). Such elements show that the order of magni-

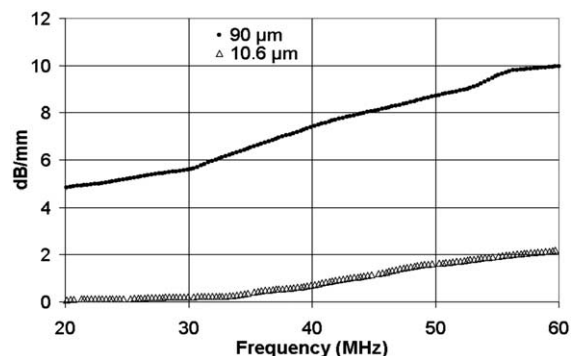


Fig. 7. Longitudinal attenuation in UO₂ as a function of frequency.

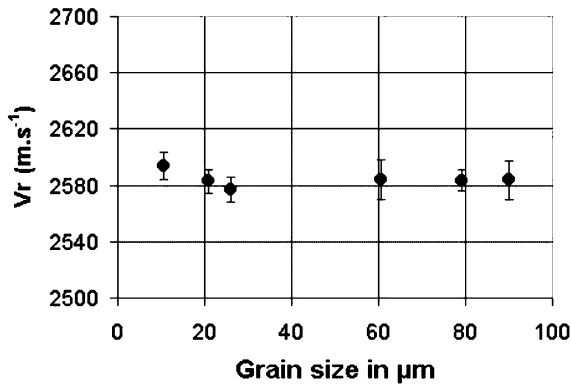


Fig. 8. Rayleigh wave velocity as a function of grain size.

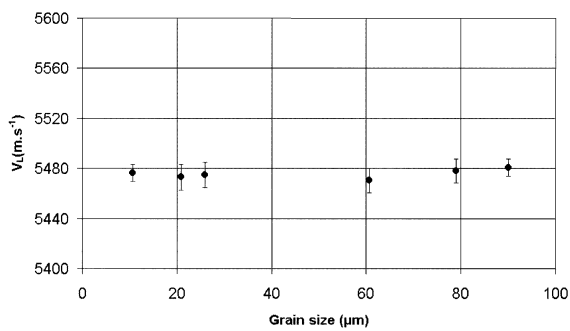


Fig. 9. Longitudinal velocity measurements in UO₂.

tude found experimentally is correct. But, using the models to perform accurate quantitative comparisons seems meaningless because many parameters used in the models are not known accurately (exact shape of the grains, anisotropy factor, ...). So, only this qualitative comment will be made in this paper.

Velocities measurements have been performed with a 15 MHz sensor in $V(z)$ and with the two 40 MHz sensors described above for longitudinal velocities assessment. As UO₂ is not a layered media, the choice of frequency has no influence on the velocities. With the relations obtained in Ref. [4] between the ultrasonic waves velocities and the porosity, the velocities have been extrapolated at 0% porosity. The results are reported on Figs. 8 and 9. The size of the grains has no influence on the ultrasonic waves velocities.

4. Conclusion

Works are going on for the application of micro-acoustic methods for UO₂ characterisation. Even if in the presentation here above the experimental work has been

done at present only on a few samples of non-irradiated UO₂ in which attenuation is not very high, we have demonstrated the interest of attenuation measurements to bring additive information. Our purpose for the future is to obtain many samples with other micro-structures: various O/M ratios, defect structures, solid solutions. In such samples sensitivity should be better.

With the attenuation parameter, new characteristics of the material (which do not affect velocities) are observed. As mentioned in introduction, the coupling between these two measurements will lead to a total evaluation of the damage state of the material. The application of such methods on irradiated material will be very interesting: velocities will provide volume fraction porosity (with the help of calibration laws established in our previous studies) and attenuation, information on all other defects (microfracturation, ...). Thanks to the local aspect of our measurements, the radial gradient of mechanical properties will be totally investigated. The measurement of attenuation could also be interesting for the analysis of the subdivision of grains in the RIM area.

References

- [1] D. Baron, J. Spino, Does Rim Microstructure Formation degrade the Fuel Rod Performance?, International IAEA Technical Committee Meeting on Technical and economic Limits to Fuel Burn-up Extension, Bariloche, Argentina, 15–19 November 1999.
- [2] J. Spino, D. Baron, D. Papaioannou, Rim formation and fission gas behaviour: some structure remarks, International IAEA/NEA Seminar on Fission Gas Behaviour in Water Reactor Fuels, Cadarache, France, 26–29 September 2000.
- [3] H. Bailly, D. Ménessier, C. Prunier, Le combustible nucléaire des réacteurs à eau sous pression et des réacteurs à neutrons rapides, Paris 5^{ème}: Eyrolles CEA, p. 670, Série Synthèses.
- [4] V. Roque, B. Cros, D. Baron, P. Dehaut, J. Nucl. Mater. 277 (2000) 211.
- [5] V. Roque, D. Baron, J. Bourgoïn, J.M. Saurel, J. Nucl. Mater. 275 (1999) 305.
- [6] E. Papadakis, Ultrasonic attenuation caused by scattering in polycrystalline media, in: W.P. Masson (Ed.), Physical Acoustics, vol. IV-part B, Academic Press, New York, 1968.
- [7] G.A.D. Briggs, Acoustic Microscopy, Clarendon, Oxford, 1992.
- [8] J.I. Kushibiki, IEEE Trans. Sonics Ultrasonics SU-32 (2) (1985).
- [9] D.R. Hull, H.E. Kautz, A. Vary, Mater. Eval. 43 (1985).
- [10] C.C. Lee, M. Lahham, B.G. Martin, IEEE Trans. Ultrasonics Ferroelectrics Frequency Ctrl. 37 (4) (1990).